Eur. Phys. J. B **9**, 551–558 (1999)

THE EUROPEAN PHYSICAL JOURNAL B

EDP Sciences

Energy dissipation in solid friction

S. Ciliberto[a] and C. Laroche

École Normale Supérieure de Lyon, Laboratoire de Physique[b], 46 allée d'Italie, 69364 Lyon Cedex 07, France

Received 9 November 1998

Abstract. Dissipation in solid friction is studied as a function of the elastic properties of the two sliding surfaces. The two surfaces have been constructed by embedding macroscopic asperities in an elastic layer. It is shown that when the surfaces are rigid the energy dissipation is smaller than in the elastic case. The scaling of the friction force as a function of the asperity number is also studied.

PACS. 46.30.Pa Friction, wear, adherence, hardness, mechanical contacts, and tribology – 05.70.Ln Nonequilibrium thermodynamics, irreversible processes

1 Introduction

Solid friction has been always widely studied for its importance in many technical and natural process. In spite of the enormous effort done to connect macroscopic effects with microscopic dynamics of asperities, many problems are still open and are a subject of current interest [1,2]. An important question, which is not jet completely understood, is how the energy is dissipated in the asperity interaction.

As proposed by Tomlinson [3], the dissipation is the consequence of the multiplicity of metastable positions for the sliding surfaces, due to the presence of the asperities. At each jump between metastable positions, a small portion of the sliding surface undergoes a displacement, during which the energy is dissipated. The same conclusion is reached in the model of independent asperities [4,5]. Similar mechanisms are often invoked to understand the friction of an AFM with a surface [6] and in the wetting of a liquid interface with a substrate [7,8].

Several numerical simulations have been done to understand how collective behaviour of many asperities may actually destroy the multistable effects and how the friction force scales as a function of the asperity number [9–12]. To check these ideas experimentally it is not easy, because friction between two surfaces changes the surface roughness and the experimental parameters may not be constant during a long experiment. Furthermore in real surfaces the asperities are small (of the order of a few microns). Thus it is very difficult to relate the jumps of the surfaces to some characteristic length. For these reasons, we decided to study the problem of the energy dissipation on artificial surfaces, previously employed in other experiments [13,14]. The advantage in using artificial surfaces is that the size of the asperities and the elastic properties of the surfaces are very well controlled. From this point of view the experiment can be seen as an analogic simulation of the interaction of two rough surfaces. However the fact, that in a real experiment other sources of friction could mask the multistable mechanism, makes the results of these experiments more close to a real experiment of friction. Furthermore, friction, between these two artificial surfaces, presents an interesting and complex dynamics, which has been described in references [13–15]. Thus it is interesting to study the dissipation mechanisms of these surfaces.

In this paper we show that the jumps among metastable positions are the most important source of dissipation, if the surface compliance is the largest one in the experimental set-up. In these experiments we can measure the force induced by a single asperity and the energy dissipated in a jump as a function of the surface compliance.

The paper is organised as follows: in the next section the experimental set-up is described, in Section 3 the single asperity case is discussed, the results with the interaction of many asperities are described in Section 4. Finally we conclude in Section 5.

2 The experimental set-up

The experimental set up, shown in Figure 1, is a modified version of those of references [13,14]. A slide of 10 cm long and 10 cm wide is moved at constant speed V in the x direction on a track with a rough surface. The motion of the slide is maintained straight by two guides which avoid the lateral motion. The rough surfaces of the slide and of the track are constructed by embedding metallic spheres of radius $R = 3$ mm in elastic layers with different stiffness. For technical reasons the spheres of the slide are made of bronze whereas those of the track are made of steel. The spheres emerge of about 2 mm from the layer

[a] e-mail: cilibe@physique.ens-lyon.fr
[b] CNRS URA 1325

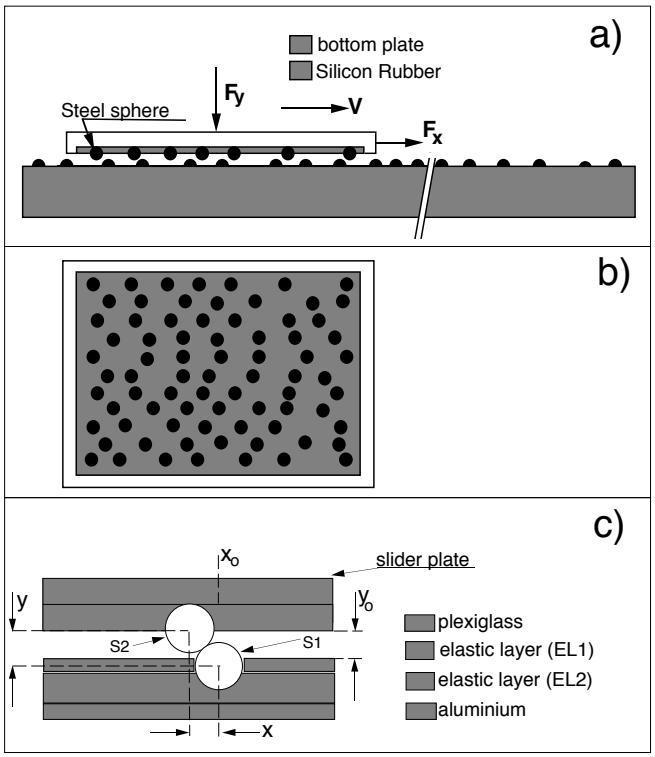

Fig. 1. (a) Cross section of the experimental apparatus; the slide is moved at constant speed V and the friction dependent force F_x is measured by a force transducer. The spheres are embedded in an elastic layer. (b) bottom view of the slide. (c) Expanded view of the contact between two spheres. The spheres S1 and S2 have a radius $R = 3$ mm, y and x are respectively the vertical and horizontal distance between the sphere centres. y_o and x_o are respectively the unperturbed horizontal and vertical distances of the sphere centres. x_o is moved at constant loading speed V. The slider is made of a plexiglass plate and an elastic layer of rubber. The track is made of an aluminium base and a plexiglass plate with holes in which the sphere (S1) can move up and down. Between the plexiglass and the base an elastic layer of rubber is inserted.

surfaces. In this way an artificial surface with controlled roughness and elasticity is constructed. The maximum roughness is exactly 2 mm. The details for a single asperity are shown in Figure 1c. Each sphere is rather free to move around its equilibrium position because of the elasticity of the rubber layers. The dynamics has been studied as a function of the matrix compliance, which has been changed using materials with different elastic properties.

The system is composed by N_l lines parallel to the loading speed direction (x). As shown in Figure 1b, each line of the slide has n spheres, whereas the linear density of spheres on the track is n_d. The spheres are randomly distributed on the track surface. The values of n, n_d and N_l can be modified in the experimental apparatus, specifically $1 \leq n \leq 7$, $5\ \mathrm{m}^{-1} \leq n_d \leq 87\ \mathrm{m}^{-1}$; $1 \leq N_l \leq 11$. Thus the mean number of interacting asperities on the slide can be changed from 1 to 80. The mean distance between the sphere centres is about $4R$ at the maximum sphere density. The slide is moved at constant speed V, which can be changed in the range: $0.02\ \mathrm{mm/s} < V < 20\ \mathrm{mm/s}$.

The force $F_x(t)$ necessary to move the slide at constant speed is measured by a force transducer. The transducer signal, suitably amplified and filtered, is converted by a 16 bits A/D converter. The minimum detectable variation of the friction force F_x is about 3×10^{-2} N.

The experiment is performed at imposed distance y_o between the slide and the track. Therefore the normal force F_y acting on the surfaces fluctuates. The mean value $\langle F_y \rangle$ of F_y can be changed by modifying y_o. $F_y(t)$ is also measured by a force transducer and converted by a 16 bits A/D converter with a sensitivity comparable to the horizontal one. The experiment can be also performed at constant F_y. In such a case is y_o which fluctuates. However no significant difference between the experimental results obtained at imposed y_o and those obtained at imposed F_y has been observed. Much care has been taken in the montage to maintain a good parallelism between the slide and the track in all positions. The maximum error is around $\pm\ 0.015 y_o$.

In order to simplify the interpretation of the results we imposed a well defined displacement directions for the spheres of the track and those of the slide. Indeed when the asperity displacements are symmetric in the pushing direction and transverse directions many problems may arise, as it has been discussed in reference [5].

3 The interaction of isolated asperities

We first consider the case of two isolated asperities, which is schematised in Figure 1c. The track sphere (S1) can be displaced only vertically and is subjected to a vertical elastic force, of mean stiffness $K_y = 2.3 \times 10^4$ N/m, produced by an elastic layer (EL1 in Fig. 1c). The sphere of the slide (S2) can be displaced only horizontally in the direction of the loading speed and is subjected to a horizontal elastic force of stiffness K_x, produced by an elastic layer (EL2 in Fig. 1c). Two values of K_x has been used, specifically $K_x = 9 \times 10^6$ N/m (rigid case $K_x > K_y$) and $K_x = 5 \times 10^2$ N/m (elastic case $K_x < K_y$). A minimum distance y_o is imposed between the slide and the track, such that $R < y_o < 2R$, where R is the sphere radius. With this geometry the only way for an asperity (S2) of the slide to pass over an asperity (S1) of the track is to push down the bottom sphere S1. In Figure 1c, x and y are respectively the horizontal and vertical distances between the sphere centres. The point x_o, of the top slide frame, moves at constant speed V, that is $x_o = Vt - x_1$, where $-x_1$ is the horizontal distance at which the two spheres begin to be in contact. The coordinates x_o and y_o correspond to the unperturbed distances between the two sphere centres, that is $x = x_o$ and $y = y_o$, when the two spheres are not in contact.

3.1 The equations of motion

When the surface of S1 touches that of S2 the geometry imposes:

$$y = \sqrt{4R^2 - x^2}, \quad \text{for } |x| < x_1 \tag{1}$$

where $x_1 = \sqrt{4R^2 - y_o^2}$.

Therefore with this geometrical constraint, the interaction potential $U(x)$, between two spheres, is:

$$U(x) = \frac{1}{2}K_y(\sqrt{4R^2 - x^2} - y_o)^2, \quad \text{for } |x| < x_1$$

and $U(x) = 0$ for $|x| > x_1$. In the quasistatic regime, neglecting friction between the sphere surfaces, the total energy E_t of the two sphere system is:

$$E_t = \frac{1}{2}K_x(x_o - x)^2 + \frac{1}{2}K_y(\sqrt{4R^2 - x^2} - y_o)^2, \quad \text{for } |x| < x_1 \tag{2}$$

where $(x - x_o)$ is the horizontal stretch of the upper elastic layer.

We now briefly recall the main results of the model of reference [4]. If the stiffness K_x is very large, that is the elastic layer of the slide (EL2 in Fig. 1c) is very rigid ($K_x \gg K_y$), equation (2) has only one minimum at $x = x_o$, that is S1 remains in its unperturbed position and only S2 moves vertically. In the quasistatic regime, that is when $V \ll 2R\sqrt{K_x/m}$ (m is the sphere mass), the horizontal and vertical forces, for $|x_o| < x_1$ are

$$F_x = -\left[\frac{\partial U}{\partial x}\right]_{x=x_o} = K_y(\sqrt{4R^2 - x_o^2} - y_o)\frac{x_o}{\sqrt{4R^2 - x_o^2}} \tag{3}$$

$$Fy = \left[-\frac{\partial U}{\partial y}\right]_{x=x_o} = -K_y(\sqrt{4R^2 - x_o^2} - y_o) \tag{4}$$

with $y = \sqrt{4R^2 - x_o^2}$ and $x_o = Vt - x_1$. For $|x_o| > x_1$, when there is no interaction between the two spheres, $F_x = 0$.

In contrast when $K_x < K_y$, it can be easily shown that equation (2) has three extrema of which, two are stable and one is unstable [5]. Thus, by moving x_o, the sphere S_1 of the slider jumps from one stable point to the other. These jumps between the stable points are just the mechanism for energy dissipation in solid friction. Of course in our system part of the energy is dissipated because of friction between the sphere surfaces, but we can easily check if the amount of energy dissipated in the jumps is larger than that lost by friction between the sphere surfaces.

In practice in our system a few changes of equation (3) and of equation (4) are required. Firstly K_y is not strictly constant because when the sphere S_2 penetrates inside the rubber layer the contact area increases. The behaviour of F_y as a function of $(y - y_o)$ is shown in Figure 2. Secondly the friction coefficient ν between the sphere surfaces (bronze-steel) is not 0 but 0.1. Therefore equation (3) becomes:

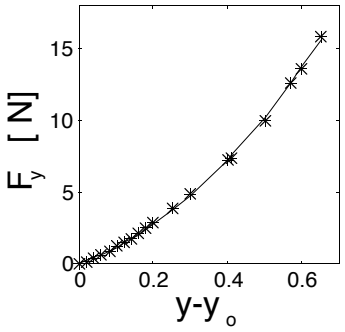

Fig. 2. The force F_y exercised on the sphere S1 by the rubber layer (EL1 in Fig. 1) as a function of the vertical displacement of S1.

$$F_x = f(y - y_o)\frac{\nu y - x_o}{y + \nu x_o} \quad \text{for } |x_o| < x_1 \tag{5}$$

where the function $f(y - y_o)$ is the best fit of the data of Figure 2.

Equation (5) corresponds to an experiment with imposed y_o. One can check another form of sphere interaction by imposing the normal force F_y and making layer 2 of Figure 1c very rigid, that is $K_y \gg F_y/R$. In such a case is the slide that will move up and down the total energy for $\nu = 0$ becomes:

$$E_t = \frac{1}{2}K_x(x_o - x)^2 + F_y(\sqrt{4R^2 - x^2} - y_o) \quad \text{for } |x| < x_1. \tag{6}$$

where y_o is now the minimum y, imposed by the external conditions. As a consequence for the rigid case ($K_x \gg F_y/R$) equation (6) has only one minimum at $x = x_o$. Then, for $\nu \neq 0$, F_x becomes:

$$F_x = F_y\frac{\nu y - x_o}{y + \nu x_o}\frac{x_o}{y} \quad \text{for } |x_o| < x_1 \tag{7}$$

with $y = \sqrt{4R^2 - x_o^2}$ and $x_o = V\ t - x_1$. $F_x = 0$ for $|x_o| > x_1$.

In the elastic case, when $K_x < F_y/R$, also equation (6) has three extrema like equation (2). Two of these three extrema are stable and one is unstable. Thus, by moving x_o, the system will jump between the two stable ones. Therefore also when F_y is imposed, one would expect that the system has to be more dissipative in the elastic case than in the rigid one.

3.2 The results at imposed y_o

We consider first the case at imposed y_o. The results of the measurements of the horizontal and vertical force produced by the interaction of two isolated asperities are plotted in Figures 3 and 4 for the rigid and elastic cases respectively.

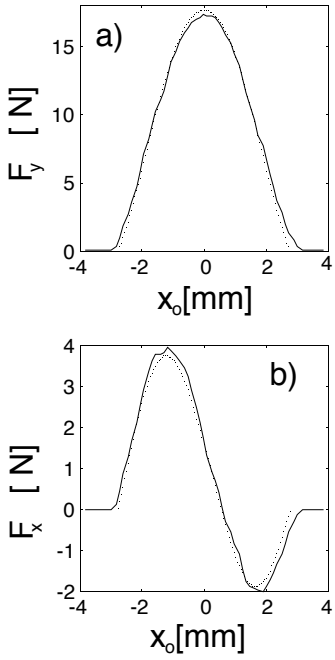

Fig. 3. The forces F_y (a) and F_x (b) between two asperities are plotted as a function of x_o for the rigid case with $K_x \gg K_y$ and $y_o = 5.3$ mm. The continuous line corresponds to the experimental measurements whereas the dotted line is obtained from equation (5) with the parameters given in the text.

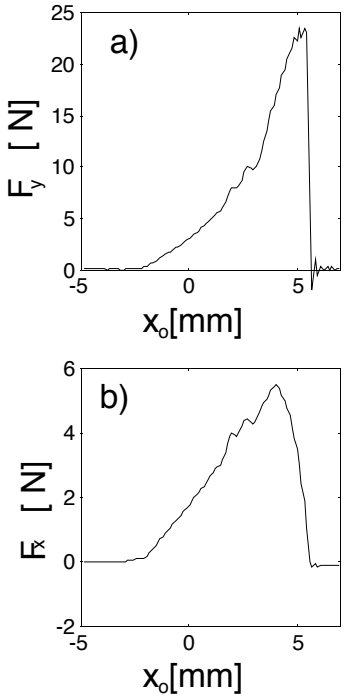

Fig. 4. The forces F_y (a) and F_x (b) between two asperities are plotted as a function of x_o for the elastic case with $K_x < K_y$ and $y_o = 5.3$ mm.

In Figure 3b the force F_x is shown as a function of x_o for the rigid case ($K_x \gg K_y$). We clearly see that the shape of the potential derivative 3 is well reproduced except for a negligible asymmetry produced by the friction between the two sphere surfaces. This asymmetry is perfectly taken into account by the F_x obtained from equation (5).

In Figure 4b the force F_x is plotted as a function of x_o, for $K_x < K_y$ (elastic case). We clearly see that the negative part of the force is totally erased, therefore the dissipation is larger in the elastic case than in the rigid one, that is energy is mainly dissipated in the asperity jumps.

The energy dissipated in the passage of the sphere S2 over S1, both in the rigid and elastic case, can be estimated, by computing the work W_o done by the force F_x. The results for a single asperity are shown in Figure 5 where W is plotted as a function of the normal load, which is simply changed by changing y_o. We clearly see that W_o is much larger in the elastic case that in the rigid one. Thus at least for two isolated asperities we observe that the jumps between metastable positions strongly increase the energy dissipated during the interaction between the two asperities.

3.3 The results at imposed F_y

The same effects are observed if F_y is imposed instead of y_o. The results are shown in Figure 6 where F_x measured as a function of x_o during the interaction of two asperities. In the rigid case, Figure 6a, we see that the curve is very well fitted by the prediction done using equation (7). In contrast in the elastic case, Figure 6b, we immediately see that the energy dissipation is higher than in the rigid case, because the negative part of F_x *versus* x has been completely erased by the sphere jump. This is quite interesting, because we see that independently of the interaction potential the elastic case is always more dissipative of the rigid one.

4 The interaction of many asperitites

We now consider the case of many asperities because collective effects may actually destroy the existence of this multiplicity between metastable positions. Thus we have studied how the forces F_x and F_y change as a function of the asperity density ρ on the track surface. This has been done in such a way that the interaction potential between the single asperities remain constant, when the number of asperity is increased. The best way to achieve this result is to make the experiment imposing the distance y_o between the two surfaces.

4.1 Asperity density dependence

In our experiment the value of ρ can be modified by changing n_d and N_l, specifically $\rho = (n_d N_l)/N_{max}$, where $N_{max} = 957$ m^{-1} is the maximum of the product $(n_d N_l)$. As an example of the force evolution at $\rho = 0.52$ and $y_o = 5.1$ mm we plot F_y and F_x as a function of x_o for the rigid case in Figures 7a, c and elastic case, Figures 7b, d. We

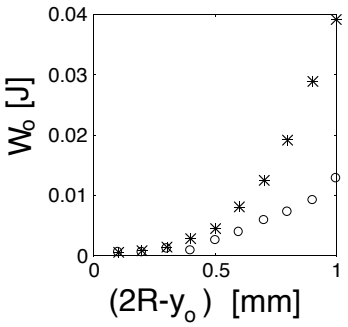

Fig. 5. Dependence on y_o of the energy W_o dissipated by two asperities.

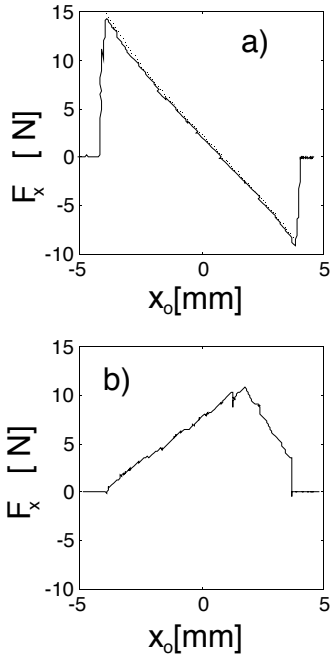

Fig. 6. The force F_x between two asperities with an imposed $F_y = 20$ N is plotted as a function of x_o for the rigid (a) and elastic case (b). The dotted line in (a) is obtained from equation (7) with $\mu = 0.11$.

see that the evolution of the force is quite different from that of two isolated asperities. The forces F_x and F_y fluctuate around a well established mean value $\langle F_x \rangle$ and $\langle F_y \rangle$ respectively. We have also computed the relative r.m.s. fluctuations σ_a of F_a, that is $\sigma_a = \sqrt{(\langle F_a^2 \rangle / \langle F_a \rangle^2) - 1}$.

We have studied how the mean forces $\langle F_x \rangle, \langle F_y \rangle$ and the relative fluctuation amplitudes σ_x, σ_y change as a function of ρ. The mean horizontal force $\langle F_x \rangle$ is plotted as a function of ρ in Figure 8a at fixed y_o. The corresponding mean values of F_y are instead plotted in Figure 8b. The mean values grow as a function of ρ both for the rigid and elastic cases, but the frictional force is always larger for the elastic case than for the rigid one, whereas the mean values of $\langle F_y \rangle$ remain comparable in the two cases.

The relative r.m.s. fluctuations σ_x and σ_y are instead plotted as a function of ρ in Figures 8c, d respectively. The relative fluctuations of F_x and F_y decrease as a function of the asperity number. In Figure 9a, b, σ_y and σ_x are plotted as a function of ρ in a log-log scale. The straight continuous lines, which are traced for reference, represent the function $\rho^{-1/2}$. We see that σ_y and σ_x decrease, for small ρ, roughly as $\rho^{-1/2}$. For increasing ρ the behaviour of σ_y and σ_x as a function of ρ becomes more complex. This shows that for small ρ, that is when the distances among asperities are much larger than $2R$, the asperity jumps are almost uncorrelated. Whereas when the asperities begin to be close a certain degree of correlation exists and the jumps are not totally independent. This fact, which was already discussed in reference [9] has a very important consequence, when one tries to estimate the friction force for many asperities starting from the value estimated from a single asperity.

4.2 Comparison with models

Indeed the value of the energy W_o dissipated in a single jump could be used to estimate how the tangential force grows when the number of asperities is increased. If the asperities are independent then, from the model of reference [4], one obtains for the total tangential force:

$$\langle F_x \rangle = N_{\max} \rho n W_o. \tag{8}$$

The force should increase linearly as a function of ρ. In Figure 8a the continuous line is computed from equation (8), using the value of W_o measured for the single asperity. We clearly see that the measured values are lower than the computed ones even for the elastic case. This is due to the asperity coupling, which reduces the amplitude of the asperity jumps. Furthermore the dependence of F_x on ρ is far to be linear. However what is very important to notice here, is that even in presence of many asperities F_x in the rigid case is smaller than in the elastic one.

In Figure 10a we show the measured values of F_x as a function of ρ in a log-log scale. Also the measurements done at constant F_y are reported. We clearly see that F_x increases as a power law both for the rigid and for the elastic case, that is:

$$F_x \propto \rho^{\gamma} \tag{9}$$

with $\gamma \simeq 0.66 \pm 0.03$ both for the rigid and elastic case. This fit is shown also in Figure 8a as a dashed line and the agreement is quite good. The value of the exponent γ has been predicted in a recent paper [9] and takes into account the fact that not all the asperities are independent, but a certain degree of correlation among jumps exists. This is consistent with the behaviour of σ_x and σ_y as a function of ρ, which we discussed in the previous section.

Finally we have computed the friction coefficient μ between the two rough surfaces as the ratio between $\langle F_x \rangle$ and $\langle F_y \rangle$. The value of μ as a function of ρ are reported in Figure 10b. The mean value of μ is about 0.3 for the elastic case and 0.13 for the rigid case. We see that the value for the rigid is close to the value of the bronze-steel friction whereas the presence of an elastic matrix strongly increases the dissipation.

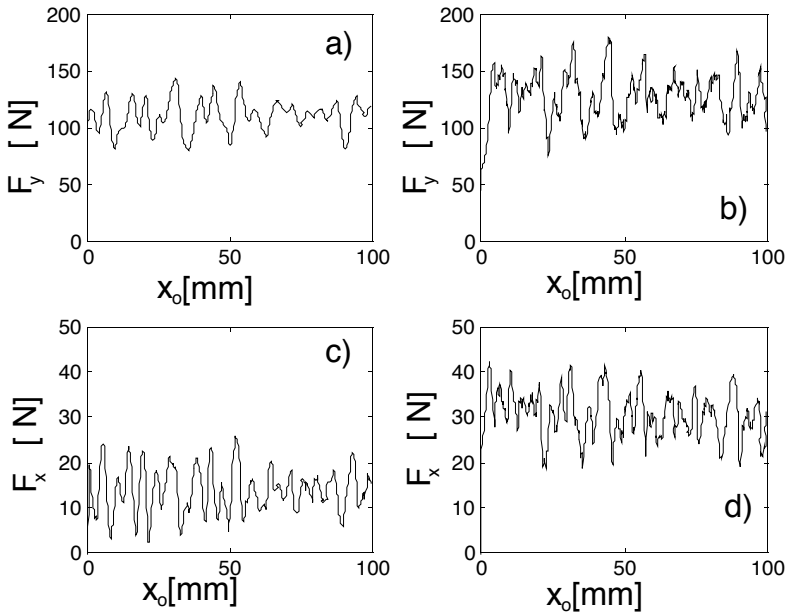

Fig. 7. Force F_y between many asperities as a function of x_o for the rigid (a) and elastic cases (b) at $\rho = 0.52$ and $y_o = 5.1$ mm. The corresponding F_x are plotted as a function of x_o in (c) and (d) for the rigid and elastic cases respectively.

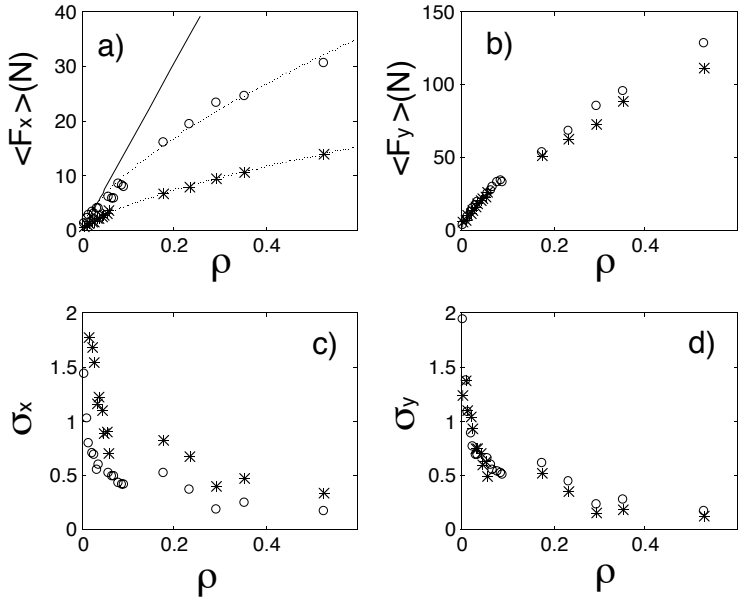

Fig. 8. The forces F_x (a) and F_y (b) are plotted as a function of the asperity density ρ at $y_o = 5.1$ mm and $V = 0.1$ mm/s. The symbols ($*$) and ($\circ$) correspond to the rigid and elastic case respectively. In (a) the dotted lines are the prediction of equation (9) whereas the continuous straight line is obtained from equation (8). The dependence on ρ of the relative fluctuations σ_x and σ_y is shown in (c) and (d) respectively.

4.3 Velocity dependence

It has been predicted that the energy dissipated in the interaction of two isolated asperities scales for $V \to 0$ as $V^{2/3}$ [16,17]. We checked this dependence both for the rigid and for the elastic cases. The results are shown in Figure 11a where μ is plotted as a function of $V^{2/3}$ and in Figure 11b where μ is plotted as a function of V in a log-log scale. We see that the growth of μ with velocity is confirmed. However the $V^{2/3}$ law can be well fitted only for a single asperity in the elastic case, for very small velocities. In the rigid case, with only two isolated asperities, we see (Fig. 11b) that a logarithmic dependence on V is clearly much better. The same behaviour is observed for the elastic case with many asperities, as can be seen in Figure 11b. Thus in our system the friction coefficient seems to have a logarithmic dependence on V instead of the predicted dependence. The reason of this discrepancy

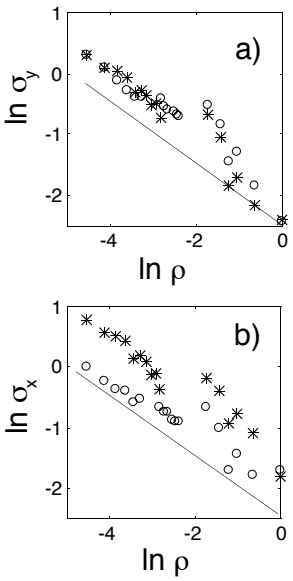

Fig. 9. Dependence on ρ of the relative fluctuations σ_y (a) and σ_x (b) in a log-log scale. The continuous line corresponds to the function $\rho^{-1/2}$.

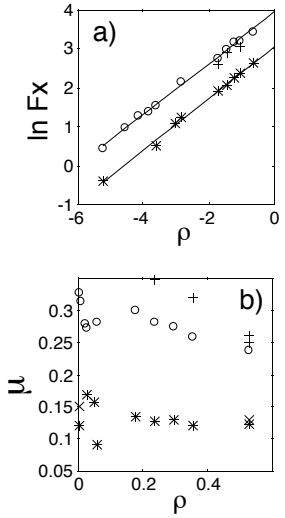

Fig. 10. (a) The dependence of F_x on ρ in a log-log scale. The continuous straight lines are the power law predictions of equation (9). (b) Friction coefficient as a function of the asperity density The symbols ($*$) and ($\circ$) correspond respectively to the rigid and elastic case for imposed y_o, whereas crosses correspond to the elastic case with imposed F_y.

is unclear, but it is probably related to the fact that the simple hypothesis of the model [16,17], are not totally respected by the vertical dynamics of our system. Indeed in the model, the interaction potential is velocity independent. This is not the case in our system because of a certain degree of viscoelasticity of the rubber layers, used in the experimental set-up.

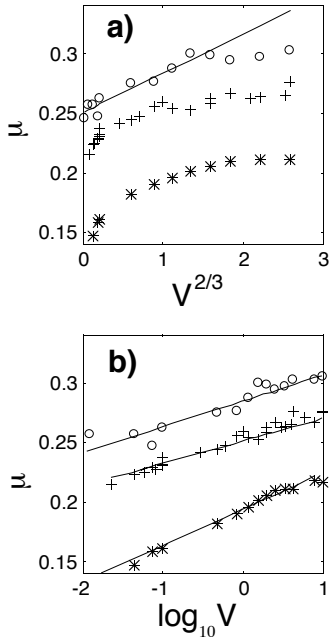

Fig. 11. The dependence of F_x on V for the single asperity in the elastic (o) and rigid ($*$) cases. The symbols ($+$) correspond to the elastic cases with $\rho = 0.52$. In all of the experiments $y_o = 5.3$ mm.

5 Conclusions

We have analysed the energy dissipation mechanisms of two surfaces with macroscopic asperities. The tangential force between these two surfaces have been studied as a function of the surface compliance using two types of interaction potential among asperities. This set of measurements shows that, as predicted by simple models [3,4] of solid friction, energy is dissipated in the asperity jumps between metastable positions. This is true not only in the case of a single asperity but also in a system composed by many asperities. We have studied how the tangential force between the two surfaces depends on the density of the asperities. As discussed in reference [9], the asperity coupling reduces the amplitude of the jumps and the amount of dissipated energy increases slower than linear as a function of the asperity density. Indeed we have observed that the pinning force has a power law dependence on the asperity density, with an exponent of $2/3$ which has been predicted in reference [9]. The agreement between the predictions of reference [9] and these experimental analysis shows that the analysis of reference [9] is useful in describing the dynamics of our artificial surfaces, which presents instabilities involving a large number of particles [13]. We also recall that these surfaces have a recovery length [14] which also agrees with the results of reference [9]. The experimental results on the recovery length described in [14] show a strong analogy with the motion of a contact line in the quasi static regime [7,18]. Therefore the experimental study, here described, can be very useful in order to understand the influence of disorder in the displacement of a liquid interface on a plane and the microscopic mechanisms

of solid friction, but also in the study of other phenomena, such as the friction at the tip in AFM microscope [6].

Another important effect, which has not been investigated here, is the role of three dimensional effects on the observed phenomenology. In our experiment the driving force is almost tangential to the surfaces. It will be interesting to study how the distance between the surface and the application point of the driving force may modify the results. The coupling between the driving force will be done *via* an elastic layer of a certain thickness. This study will allow us to give more insight on the coupling of the elastic deformation of the solid and that of the asperities. This point, which is not yet very well understood, could be easily studied in our system.

We acknowledge L. Bocquet, E. Charlaix and J. Crassous for useful discussion. This work has been partially supported by CEE contract n° ERBCHRXCT 940546.

References

1. B.N.J. Persson, E. Tosatti, in *Physics of sliding surfaces, Vol. 311* of *NATO Advanced Study Institut, series E*, edited by B.N.J. Persson, E. Tosatti (Kluwer Academic publishers, Dordrecht, 1996).
2. F. Heslot, T. Baumberger, B. Perrin, B. Caroli, C. Caroli, Phys. Rev. E **49**, 4973 (1994).
3. G.A. Tomlinson, Philos. Mag. **7**, 905 (1929).
4. C. Caroli, P. Nozières, in *Physics of sliding surfaces, Vol. 311* of *NATO Advanced Study Institut, series E*, edited by B.N.J. Persson, E. Tosatti (Kluwer Academic publishers, Dordrecht, 1996).
5. A. Tanguy, P. Nozières, J. Phys. I France **6**, 1251 (1996).
6. *Micro and Nanotribology and its applications, in Proceedings of the NATO-ASI conference* (1996).
7. J. Crassous, J.L. Loubet, E. Charlaix, Phys. Rev. Lett. **78**, 2425 (1997).
8. J.F. Joanny, P.-G. de Gennes, J. Chem. Phys. **81**, 552 (1984).
9. L. Bocquet, H.J. Jensen, J. Phys. I France **7**, 1603 (1997).
10. A. Tanguy, S. Roux, Phys. Rev. E **55**, 2166 (1997).
11. T. Gyalog, H. Thomas, Europhys. Lett. **37**, 195 (1997).
12. M.G. Rozman, M. Urbackh, J. Klafter, Phys. Rev. Lett. **77**, 683 (1996).
13. S. Ciliberto, C. Laroche, J. Phys. I France **4**, 223 (1994); Nonlinear Processes Geophys. **2**, 121 (1995).
14. J. Crassous, E. Charlaix, S. Ciliberto, C. Laroche, J. Phys. II France **7**, 1745 (1997).
15. S. Ciliberto, E. Charlaix, J. Crassous, C. Laroche, in *Friction and Arching*, edited by D.E. Wolf, P. Grassberger (World Scientific, 1997).
16. E. Raphael, P.-G. de Gennes, J. Chem. Phys. **90**, 7577 (1989).
17. A. Tanguy, Ph.D. thesis, University of Paris VII, France (1998).
18. J. M. Georges, A. Tonck, J.L. Loubet, D. Mazuyer, E. Georges, F. Sidoroff, J. Phys. II France **6**, 57 (1996).